Detection of Cranial- Facial Malformations: Towards an Automatic Method

Hiba Chelbi   *chelbi.hibatollah@yahoo.fr*
National Engineering School of Tunis
University of Tunis ElManar

Manel Laajimi   *laajimimanel@yahoo.fr*
National Engineering School of Tunis
University of Tunis ElManar

Wala Touhami   *wala.touhami@gmail.com*
National Engineering School of Tunis
University of Tunis ElManar

Nawrès Khlifa   *khalifa_nawres@yahoo.com*
National Engineering School of Tunis
University of Tunis ElManar

Abstract

This paper presents an original method to detect malformations in cranial facial 3D images. This is a hard task because of the complex structure of the cranium. The method is composed by several stages containing essentially a segmentation phase to localize the bone structure, a 3D image characterization to delineate automatically geometrical characteristics from the segmented images. These need to possess a mathematical definition in order to be calculated and an anatomical pertinence to be representative of the structures' shape. So, the characteristics retained are the crest lines. And finally a registration phase to identify the deformations place. This method is tested on real and synthetic data and has proved his performance.

Keywords: Cranial Malformations, HMM Segmentation Method, Crest lines, Mesh Simplification, ICIP Registration

1. INTRODUCTION

Whether they have a congenital or a traumatic origin, cranial traumas are a real health problem. Indeed, they represent one of the main causes of mortality in many countries. Of course, the continued technological development of scanner stations' keeps helping maxillary-facial surgery in the accurate analysis of these malformations. However, the complex structure of the human skull raises a problem in the detection of these malformations as well as in the diagnosis and planning of the surgical operations. To make easier this task, doctors generally used anatomical atlases which offer promising solutions.

An anatomical atlas represents a reference model taken from several individuals. It takes into account as much the resemblances as the diversities between the subjects. The atlas is generally similar to a map describing the shape, the size and the location of the structures, the identification of the deformation and the planning of interventions. Besides medicine, the atlas was used in other fields such as archeology to follow up the evolution of the skull from the prehistoric to the modern man. Unfortunately, the automatic creation of an atlas is not as obvious as it was thought. Indeed, its creation requires the manipulation of a large image base representing all possible variabilities. These images are, later on, represented by a reduced set of characteristics. We can, then, compute the average of the characteristics in order to represent the atlas. In practice, many researchers choose, with the help of an expert, an image

representing a normal anatomy and refer to it as atlas. This method could, however, be automated.

The common method to create automatically an atlas consists in few steps:

- 3D images characterization

- Identification of common characteristics.

- Modeling of common characteristics.

- Analysis of variability of common characteristics

In this work, we present the nucleus of a method aiming at the automatic creation of an atlas of the Tunisian population's skull. We validate the first stages of this method on real data in order to detect globally the maxillary-facial malformations. The following part of this paper will be organized as follows: We start with a presentation of the different stages of the chain we propose, then, we detail each stage separately before presenting and discussing the obtained results.

2. THE PROPOSED METHOD

For the creation of the atlas, we propose some stages which can be summarized in figure1.
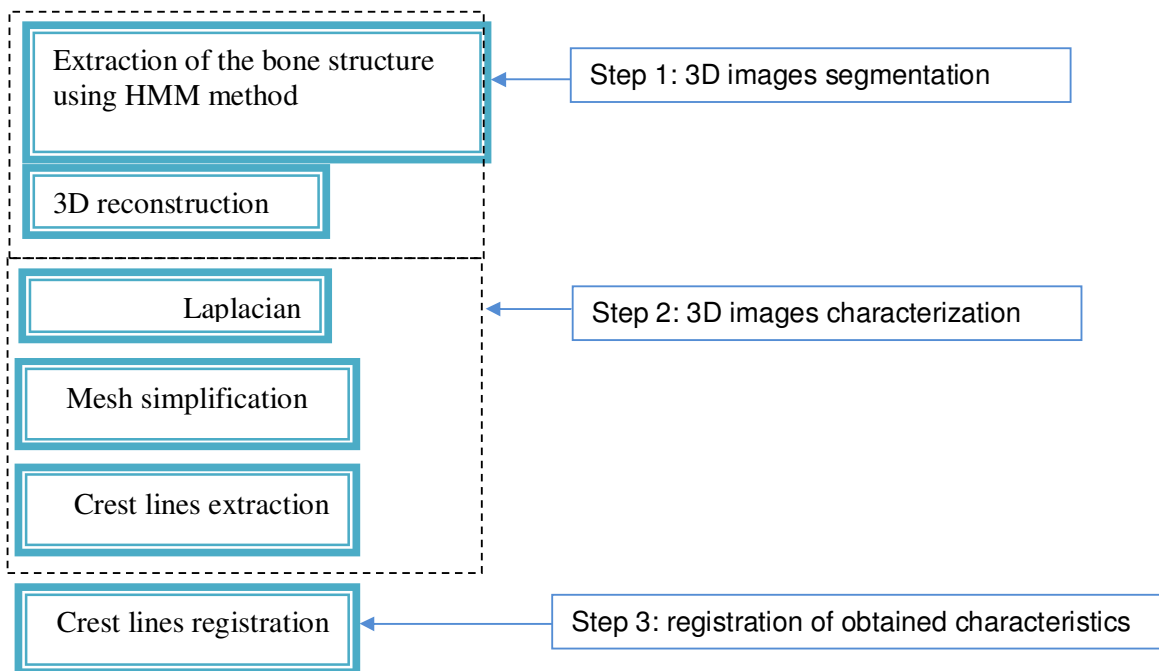
FIGURE 1: Global architecture of the proposed method

The method we propose, simple as it appears, involves some complexity at the level of choosing each technique. In what follows, we detail each step.

2.1 Extraction of the Bone Structure Using HMM Method

This first stage consists in isolating the bone structures from the remaining structures present in the skull. The manual location of these bones, though theoretically feasible, is in practice, inconceivable in reasonable times. It is, therefore, crucial to develop automatic techniques capable of providing results similar to those of an expert.

Generally speaking, the segmentation of the anatomic structures in the medical images is a particularly difficult task mainly because of both; the frequently indiscernible contours and the presence of noise. This hard aspect is increased, for the cranium CT data, due to the complex

structure of this organ. This is why the conventional methods failed to isolate the bone-structure in these images. In order to get around this problem, we propose to explore the segmentation techniques integrating a priori knowledge to guide the segmentation processes.

arkov models seems to adapt well to the segmentation problem of skull MRI scans. In fact, they introduce spatial dependence between pixels allowing segmentation robust to noise. The segmentation is performed, in a Bayesian framework, using a maximum a posteriori criteria (MAP) where the data term is modeled using a finite gaussian mixture model and the prior term is modelled by means of a hidden markov random field (HMRF). Specifically, we use the HMRF-Expectation Maximization algorithm, proposed by Zhang et al. [17]. The segmentation is fully automatic

Figure 2, presents some important results obtained by the cited method. The method performance is compared with the Otsu thresholding method generally used in isolating the bone in skull images.
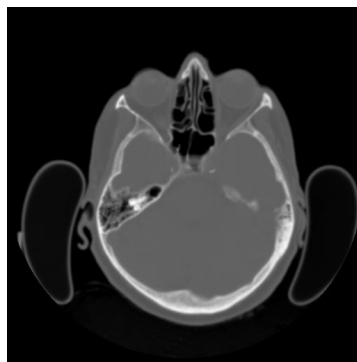
a. Original images
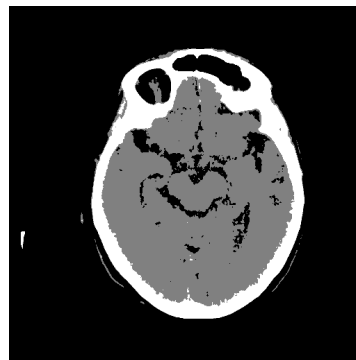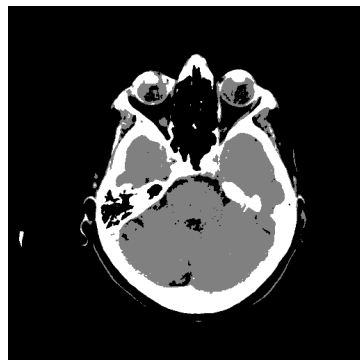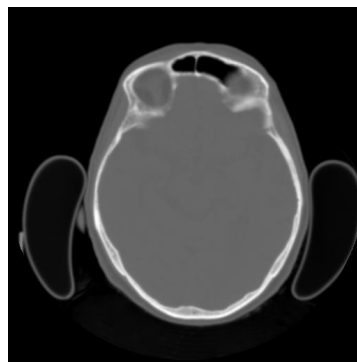
a.   Results of Otsu method
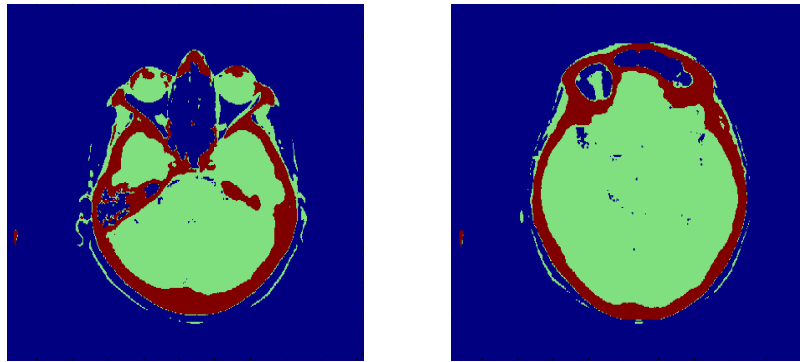
b. results of the HMM

method

FIGURE 2: Results of bone segmentation

2.2 Tridimensional Characterization of the Bone-Structures Using Crest Lines
For the creation of the atlas to be statistically significant, it is important to have a large skull image base available. Besides the problem of structural complexity related to these images, we would face the problem of the huge amount of tridimensional data to be processed. This would generate a striking complexity in the processing and analysis chain. It would so be important to represent these data through sparser but significant elements. The problem thus becomes one of tridimensional characterization with an anatomic significance.

The second stage of the proposed chain consists then in working out automatically geometrical characteristics from the segmented images. These need to possess a mathematical definition in order to be calculated together with an anatomical pertinence to be representative of the structures' shape. So, the choice of these characteristics is dependent on certain constraints. In fact, these characteristics need to be:
-   Generic: They need to be present in each one of the images of the image base.
-   Measurable: They allow a mathematical definition permitting them to be calculated.
-   Invariable: they need to have the same position in all images of the base.
-   Anatomically pertinent: they need to approve an anatomic significance as they are going to serve as a reference mark.
We finally point out that the choice of the characteristics is tightly linked to nature of the application.

Generally speaking, to characterize the volumic images, we can either characterize the volumes or the surfaces. The first case is about considering the intensity of each voxel. Given the huge number of these data (voxel), this is going to bring about very heavy and complicated calculations. In the second case, only the surface of the structures is considered. It is in this frame that our work is situated seeing that the surgical intervention is going to be operated on the external surface of the skull.
The punctual characterization consists in working out particular points which are significant and able to serve as reference. Divers points can be worked out, as it happened, the extreme ones [1] and the Harris corners [2].
The line characterization consists in calculating characteristic lines using differential geometry. As it happens, we could cite: the geodesic lines [3], the crest lines [4], the medial axes [5], the junction lines [5].

The surface characterization consists in decomposing the surface of the object into significant pieces. This method hasn't been quite used in practice, but its principle has been adopted by Clouchoux [7] to automatically define a robust fragmentation of cortical surface.
 The study of the different methods of characterization leads us to deduce that:

- The surface characteristics are difficult to manage because they include much information as they contain all the structure's points.
- In contrast, the punctual characteristics provide no more than one disparate and little robust information as there is no relationship between the points.
- The line characteristics seem to be a good compromise. Indeed, they possess at the same time a strong reduction of the information quantity together with strong connexity constraints as a line is an orderly list of points. On the other hand, the line characteristics are not all efficient: The extraction algorithms of the geodesic lines raise some problems and the median axes are unstable.

Our choice has then turned to the crest lines in order to characterize the human skull surface. Indeed, in addition to their quite simple geometrical characteristics, the crest lines involve a strong anatomic pertinence as they are very close to the "Ridge lines"; the anatomic reference marks used by doctors and which correspond to the salient structures of the skull shape.

Indeed, the anatomists locate, on the cranial structures, very specific lines called the "Ridge lines" to serve as anatomic reference marks for the maxillary facial operations. These lines correspond to the salient structures of the skull form [8]. Figure 3 presents the crest lines (in red) and the "Ridge lines" (in blue) worked out on the same skull. Both line sets are very close. They indicate that the crest lines have a strong anatomic pertinence and so are efficient for the skull characterization.
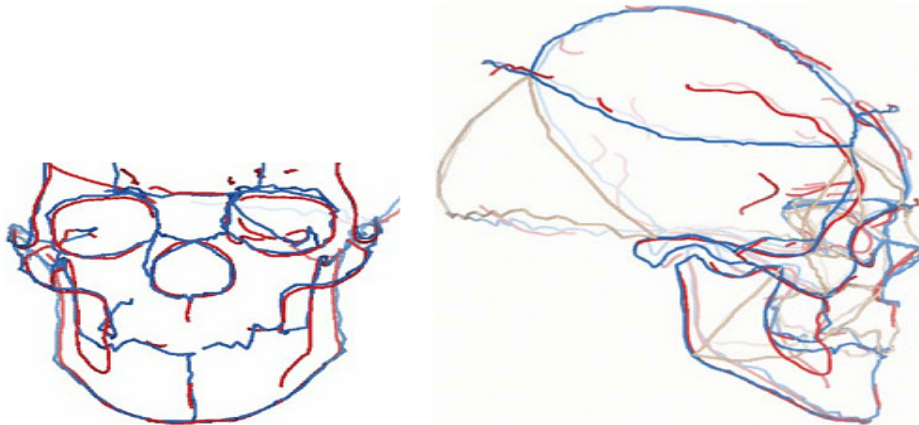
FIGURE 3: Correspondence between the crest lines (in red) and the "Ridge lines" (in blue) [8]

To work out the crest lines we are going to follow these stages. This is to guarantee that the worked out lines be usable afterwards.
- Represent the reconstructed data by a triangular grid/meshing (we use the ITK-VTK environment).
- Smooth the data with a Laplacian filtering
- Simplify the obtained mesh
- Search for the crest lines on the obtained grids.
- Filtering the set of obtained lines to keep the significant ones only.

2.2.1 Data Smoothing

The reconstructed data are unusable. Indeed, the detection of the crest lines becomes erroneous because of the detection of many which are not significant. We propose to pre-treat the raw data with a Laplacian in order to regulate them. The laplacian triangular grids operator covers practically the whole spectrum of the 3D images treatment applications including the filtering, grid, compression, configuration, segmentation and interpolation applications [9].

The Laplacian operator reduces the high frequency information in the mesh geometry. With an excessive smoothing, the important details run the risk of disappearing. A good compromise between a strong smoothing and the detection of a sufficient number of crest lines is then necessary. For the moment, we control this compromise manually, thanks to a relaxation factor

α (equation (1)). This will allow the doctor to control the number of details he wants to characterize/represent in the skull structure.

The filter used consists in adjusting the vertex's position so as to 'relax' the mesh. The new position is function of the balanced average of its direct neighbors in an iterative procedure. Indeed, the algorithm functions this way: to a given iteration i, for each point $\mathbf{p}^n_i$, a topological analysis is carried out on the vicinity N(i) to determine the points $\mathbf{p}^n_i$ which are linked to $\mathbf{p}^n_i$, and the faces which are connected to them. Then, the iterative process starts on all points. The new coordinates of the point $\mathbf{p}^n_i$ are altered according to a balanced average of the connected points with reference to the equation (1):

$$p_i^{n+1} = p_i^n + \alpha . \frac{\sum_{j \in N(i)} \alpha_{ij}(p_j^n - p_i^n)}{\sum_{j \in N(i)} \alpha_{ij}} \tag{1}$$

In this equation, alpha denotes the factor comprised between 0 and 1 which controls the displacement rate. The alpha weights can be constant or adaptive. Their calculation can be done according to several methods. For details, we cite the works [10,11]
Figure 4 gives the smoothing result with different relaxation parameters.
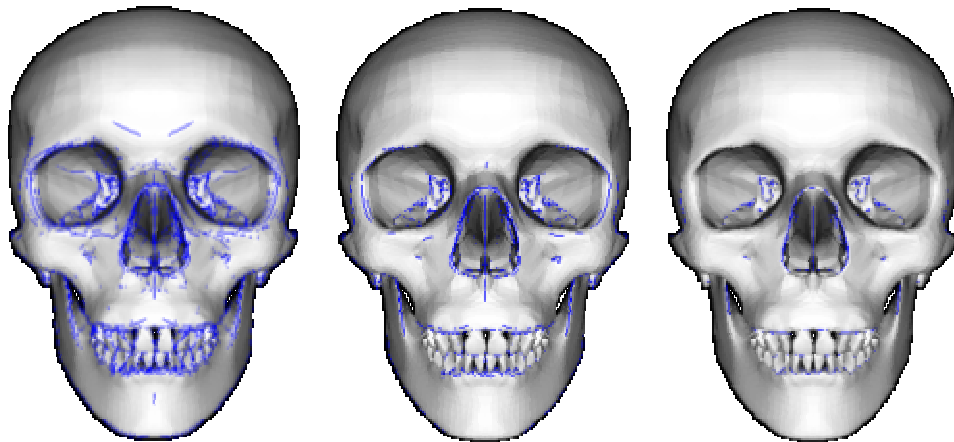
FIGURE 4: the smoothing result with different relaxation parameters

2.2.2 Mesh Simplification Phase
The obtained meshes are very dense. This could raise visualization problems and even influence the characterization quality. More generally, the grid's complexity conditions the quality of the treatments following from it. A mesh simplification stage, then, proves necessary. This amounts to a reduction of the number of the structure's polygons while preserving, in prime condition, the initial structure's topology. The mesh simplification problem is one of active research.
We remind here that we have opted for a triangular mesh this for their general aspect and their widespread use. The problem of triangular mesh simplification has been broadly studied in several works. These methods use different approaches: Edge Collapse, Vertex decimation, Vertex Clustering, Face Constriction Process.

In the first case, an edge is identified and broken down to form a new vertex. In vertex decimation, a vertex is deleted together with its borders and the whole resulting from that is re-triangulated. In vertex clustering a area is placed around the model and is divided into an equally spaced grid. The vertexes present in each cell are contracted together and

consequently the corresponding faces are updated. The process is quite fast and the exit grid's quality depends on the matrix's size. In the approaches, based on the face construction, a face is strangulated and consequently the adjacent faces degenerate and will be deleted [12-14]. For a detailed state of the art, we recommend the works of…and the references it includes. In the ITK-VTK environment, the pre-established method is that of [15] we have then opted for this solution.

2.2.3 Crest Lines Extraction Phase

The meshes are now ready to be analyzed. The following stage, then, consists in calculating the crest lines on this mesh. In the literature, several methods have been proposed to extract these lines on triangular grids.

Given that the crest lines are characterized by passing through zero of one of the curvature function's derivative. These methods are all based, in the first phase on the calculation of the curvatures. As an input, the data are meshes. All calculations are then done in the discrete domain. Several curvature estimation methods in a discrete field have been proposed. We cite by way of example: the methods using surface local parametric approximations, the curvatures are thus analytically deducted [16].The methods considering the average at the grids' faces and which approximate the curvatures in the vicinity of each vertex. The methods using the average of the curvatures' tensors curvature.Indeed, for each vortex, the curvature is taken as the tensors average of all the arrests closely related to this vortex.[16]

In what follows, we detail the curvature estimation done in the ITK-VTK environment. To do this, we used the grid's geometrical parameters represented by figure 2 which presents a face F having P as vortex: It is about the vortex P, face F's angle α_i, the length l_i of the arrest opposite the / opposed to the angle α_i and N_i the averages to the face F and β_i which represents the angle between two averages with two faces neighboring the vertex P.

From these parameters, we can calculate for each grid's vertex, its Gaussian curvature K_{Dis} given by

$$K_{Dis} = \frac{2\pi - \sum_i \alpha_i}{1/2 \sum_i Aire(F_i) - 1/8 \sum_i \cot\alpha_i l_i{}^2}$$

(2)

and its <u>average</u> curvature H_{Dis} given by :

$$H_{Dis} = \frac{1/4 \sum_i \beta_i l_i}{1/2 \sum_i Aire(F_i) - 1/8 \sum_i \cot\alpha_i l_i{}^2}$$

(3)

From K_{Dis} and H_{dis} we can deduce the maximal curvature K_{max} of the vertex such as:

$$k_{max} = H_{Dis} + \sqrt{H_{Dis}{}^2 - K_{Dis}}$$

(4)

A vertex S is considered a "crest point" only if it admits a maximal curvature kmax > 0. In fact, knowing that certain grid vertexes can have maximal curvatures with a positive value close to zero, one has to choose a value $\varepsilon > 0$ which will serve as a threshold. So, a vertex S will be interpreted as "crest point" only if it admits kmax $\geq \varepsilon$. The set of points found constitutes the grid's "crest points". The crest lines will be the arrises whose vertexes are the crest points.

2.3 Data Registration

In a subsequent stage, we will try to detect the potential malformations going solely by the characteristics calculated beforehand. This is done by registration the lines of each subject against those of the base subject.

The registration method used is the algorithm ICP (for "iterative closest point")[17.] This algorithm has been kept for its simplicity and its performance. It allows the registration of two

surfaces iteratively: to each iteration, the corresponding points (the closest points) of both entities to be registered are first defined; the average distance between the points pairs previously defined is then brought to minimum through a rigid transformation. Let P and X be two sets. The both point clouds to be registered.

Two subsets of these entities, respectively {pi} and {yi}, are put into correspondence through a similarity criterion. The matter, then, at issue is to find a rigid transformation marked (R,t) which will minimize the criterion to the meaning/in the direction of the following minimal squares:

$$e(R,t) = \frac{1}{N} \sum_{i=0}^{N} \left\| (Rp_i + t) - \psi(p_i) \right\|^2$$

(5)

where the ψ function associates to each point pi a point from the set X and N corresponds to the number of point pairs/couples. To an iteration k of the calculation procedure, the global

transformation is updated incrementally as follows. $R = R_k R$ and $t = t_k + t$

Finally, the criterion to be minimized becomes:

$$e(R_k, t_k) = \frac{1}{N} \left\| R_k (Rp_i + t) + t_k - \psi(p_i) \right\|^2$$

(6)

The correspondence function ψ is defined by:

$$\psi(p_i) = x \left| \min_{x \in X} \right| D((Rp_i + t), x)$$

(7)

Once the flunking has been performed / completed, the comparison of the two facial surfaces will be based on the appropriate point pairs in both point clouds. This allows detecting the areas of the face mass containing malformations by locating the places where the crest lines of both subjects present striking discrepancy

3. TESTS AND RESULTS

We tested the suggested method on two sets of data: the first one contains malformations were simulated by translation and rotation, the second one contains real data.

3.1 Detection of Malformations of the Simulated Data

We devote this section to the study of possible malformations which the subjects of the simulated database have. To do this, we registrate (put in correspondence) each one of these subjects to the reference image. This will enable us to define the deformed zones for each cranium. The results obtained are presented by the figure 3-a where we present the image of reference by opaque surface and those of the patients by a transparent color. To define the deformed zones, we refer to a preexistent image of Atlas. The analysis of the figure enables us to deduce that:

– The first subject, on which we did not make many modifications, does not have any malformation except for some light shifts which we cannot interpret them like malformations

– The second subject is shifted compared to the image of reference, in its frontal, zygomatic and nasal bone,

– The third subject presents even more deformations than the second since a shift in the left vertical branch of its mandible was detected.

In order to validate the performance of the results of the method, we put in correspondence the ridge lines extracted from each subject compared to those of the image of reference. The result is given by the figure 3-b, highlighting that:

– The lines of the first subject, considered as healthy, are very close even coincided with those of the reference,

– The ridge lines of the second and third subjects are shifted on certain levels.

Referring to the figure 3-a, we can confirm that we succeeded in detecting same malformations as those identified by using the whole images. Indeed, we could detect the presence of malformations, for the second and the third subjects, each one in their frontal, nasal and zygomatic bones and a malformation in the left vertical branch of the mandible of the third subject.
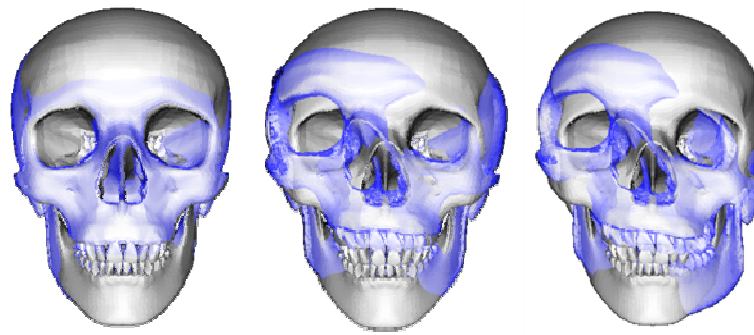
(a) Registration of images
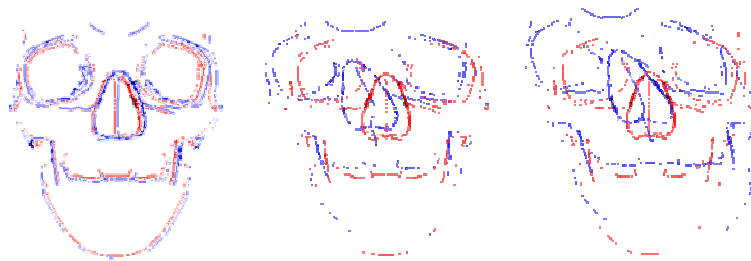
(b) Registration of crest lines

FIGURE 5: Results on simulated data

3.2 Detection of Malformations of the Real Data

Since the images of database correspond to only healthy cases, we will registrate two images by choosing one of them like reference. The result is given by the figure 4-a. As already mentioned, the two subjects are healthy, which justifies that the registration of two craniums did not give great deformations except for those due to the essential difference between the two patients. This result also is obtained, as illustrated by the figure 4-b, by registrating the ridge lines (represented by different colors), of the two subjects. This figure highlights that the two whole of lines is very close. This shows that any of the subjects does not have malformations compared to the other subject.
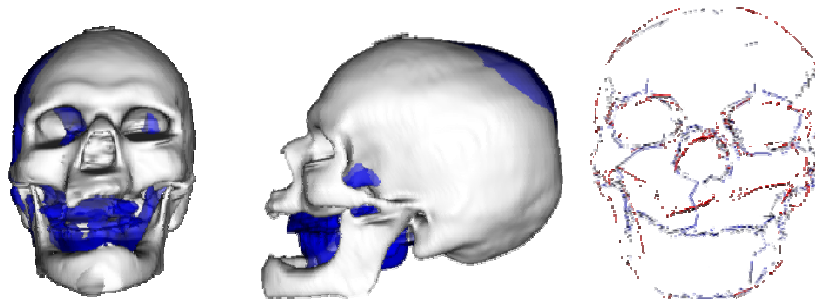
(a) Registration of real craniums   (b) Registration of crest lines

FIGURE 6: Results on real data

3. CONCLUSION

This work presents a contribution to the analysis of deformations of the scanographic images for the detection and the localization of the malformed areas of the maxillo-facial mass. The study of the normality of a subject compared to a model of reference constituted the main axis of our work. In order to manipulate heavy volume data, we extracted from the cranial images a whole of linear characteristics called "ridge lines". This choice is justified by the simplicity of these lines and their anatomical relevance. Then, we tried to detect possible malformations by registrating (putting in correspondence) the ridge lines of a subject in those of a model of reference. The results obtained by applying this method, succeed to identify the various pathological areas of the maxillo-facial mass while manipulating data of more condensed sizes and to show consequently the validity of the suggested approach in this work.

REFERENCES

[1]   C. Zhang, T. Chen, "Efficient feature extraction for 2D/3D objects in mesh representation", Proc. of the International Conference on Image Processing (ICIP), vol.3. 2001.

[2]   C.Harrisand M.J.Stephens. A combined corner and edge detector. In Alvey Vision Conference, pages147–152,1988.

[3]   J.A. Sethian et R. Kimmel, "Computing Geodesic Paths on Manifolds", Proc. Natl. Acad. Sci., 95(15):8431–8435, 1998

[4]   J-P.Thirion and A.Gourdon. The 3d marching lines algorithm. Graphical Models and Image Processing, 58(6):503509,November1996.

[5]   H Blum. A transformation for extracting new descriptors of shape . Models for the perception of speech and visual form, 1967

[6]   Hahn, M., Kr¨ uger, N.: Junction detection and semantic interpretation using hough lines. In: DAGM 2000

[7]   C. Clouchoux, O. Coulon, J-L. Anton, J-F. Mangin, J. Regis, "A new cortical surface parcellation model and its automatic implementation", in: LNCS - Medical Image Computing and Computer-Assisted Intervention - MICCAI 2006: 9th International Conference, R. Larsen and M. Nielsen and J. Sporring, n° 4191, pp. 193-200, octobre 2006

[8]   Thirion J.P., 1996b The Extremal Mesh and the Understanding   of 3D Surfaces,   in International Journal of Computer Vision, 19(2):115-128.

[9]   Max Wardetzky, Saurabh Mathur, Felix Kälberer, Eitan Grinspun, Discrete Laplace operators: No free lunch. Symposium on Geometry Processing, 2007, pp. 33-37. Laplacien

[10]   SORKINE O.:Laplacian mesh processing. State of The Art Report. Eurographics 2005),53–70

[11]   Olga Sorkine, "Differential Representations for Mesh Processing". Computer Graphics Forum, Vol. 25(4), 2006.

[12]   D. P. Luebke.: A Developer's Survey of Polygonal Simplification Algorithms. IEEE Computer Graphics and Applications'01, 24-35, (2001)

[13]   Jerry O. Talton. A Short Survey of Mesh Simplification Algorithms. University of Illinois at Urbana-Champaign, October 2004.

[14] Sajid Hussain, Håkan Grahn, and Jan Persson, "Feature-preserving Mesh Simplification: A Vertex Cover Approach," Proc. of the IADIS International Conference on Computer Graphics and Visualization 2008 (CGV 2008), pages 270-275.

[15] W. Schroeder, J. Zarge, and W. Lorenson, "Decimation of Triangle Meshes," Computer Graphics (Proc. Siggraph 92, vol. 26, ACM Press, New York, 1992, pp. 65-70.

[16] R. V. Garimella and B. K. Swartz, "Curvature Estimation for Unstructured Triangulations of Surfaces", Los Alamos National Laboratory, 2003

[17] Y.Zhang, M. Brady, and S. Smith, "Segmentation of brain MR images through a hidden Markov random field model and the expectation-maximization algorithm", IEEE Transaction on Medical Imaging, vol. 20, no. 1, pp. 45–47, 2001.